

Convection Correlations at High Re Numbers for Cavities of Cylindrical Roller Bearings

S. Guenoun¹, A. Baïri¹, N. Laraqi^{1,2}, J.M. García de María³
J.G. Bauzin¹ and A. Hocine¹

Abstract: Roller bearings are used in mechanical setups to reduce rubbing. In some applications, the thermal dissipation involved mostly due to friction between rollers and rings is important. Correct operation of the roller is possible only if local thermal phenomena are controlled. In this work, the resulting dynamical and thermal fields within the enclosures limited by rollers and rings in cylindrical bearings are obtained through numerical modelling. Convective heat transfer is quantified by $Nu-Re-Pr$ correlations for various dynamical and thermal configurations of the bearing. Two specific shape factors of the cavity and common fluids of engineering interest are considered, including air, water and a specific oil. The proposed correlations complement those existing in the specialized literature concerning the cylindrical roller bearings. They are proposed for a wide range of Re including large values and can be applied in many engineering fields.

Keywords: Convection, cylindrical roller bearing, numerical study, cavity, $Nu-Re-Pr$ correlations, high Re

Nomenclature

A	shape factor, $A = L/R$, (-)
a	thermal diffusivity, m^2s^{-1}
C_p	specific heat at constant pressure, $J.kg^{-1}K^{-1}$
D	viscous dissipation term, Wm^{-3}
k, p, n, s	coefficients of the correlation $Nu = Nu_0 + k.A^p.Re^n.Pr^s$
L	distance between consecutive rollers axis, m

¹ University Paris 10, Laboratoire Thermique Interfaces Environnement (LTIE) EA 4415 Département GTE; 50 Rue de Sèvres, F-92410 Ville d'Avray, France.

² Corresponding author: Phone + 33 (0)610540269; nlaraqi@u-paris10.fr, nlaraqi@gmail.com

³ Universidad Politécnica de Madrid, Departamento de Física Aplicada, Ronda de Valencia, 3, E-28012 Madrid, Spain.

M	number of mesh elements, (-)
Nu	Nusselt number, (-)
Nu_0	value of Nusselt number for a roller at rest (-)
P	pressure, Pa
Pr	Prandtl number, (-)
q	heat flux density, Wm^{-2}
R	radius of the roller, m
Re	Reynolds number, (-)
T	temperature of the fluid, K
T^*	dimensionless temperature of the fluid, (-)
T_0	temperature of the rings, K
\bar{T}_r	average temperature of the roller, K
$T_{max,r}$	maximum temperature of the roller, K
$T_{max,r}^*$	dimensionless maximum temperature of the roller (-)
U	velocity, $m\ s^{-1}$
V	translation velocity, $m\ s^{-1}$
X_i	coordinates

Greek Symbols

λ	thermal conductivity of the fluid, $Wm^{-1}K^{-1}$
μ	dynamic viscosity, Pa.s
ν	kinematic viscosity, m^2s^{-1}
ψ^*	streamline function
ρ	density of the fluid, $kg.m^{-3}$
ω	angular velocity, $rd.s^{-1}$
θ	angle, rd

1 Introduction

The control of thermal phenomena is fundamental for the conception of rollers which are often used in mechanical setups to decrease rubbing. In some applications, the thermal dissipation involved is significant. It is then necessary to control heat transfer to ensure correct working of the equipment. Many works deal with solids submitted to heat sources. The approaches are analytical [Patula (1981); Gecim and Winer (1986); Baïri *et al.* (2004); Laraqi (2010); Belghazi *et al.* (2010)] or numerical [Laraqi *et al.* (1994)]. Patula (1981) studied heat transfer in a cylinder exposed to a heat flux on a portion of its periphery, the rest being cooled by convection. Using the variables separation method, the author established a solution to

determine the temperature in quasi steady state regime. Gecim and Winer (1986) studied temperature distribution for the same problem using the integral transforms method. The heat diffusion in a roller was studied by considering axial heat exchanges through a surface conductance [Laraqi *et al.* (1994)]. A three-dimensional analytical model was developed to calculate the steady state temperature in a bearing ball [Baïri *et al.* (2004)]. Briot (2001) studied experimentally the influence of velocity and pressure on the temperature using a surface conductance. Two heat transportation modes are identified through rolling elements. The first one is linked to roller orbital movement (orbital transportation) around the shaft. The second one is linked to the rotating movement around its own axis in double contact zone. On the other hand, fluid behaviour into the roller has been studied in a few works. Fruman *et al.* (1996) analyze the fluid dynamics into the roller through velocity, flow and pressure measurements. In that study, velocity fields are measured by laser velocimetry. Other works treating the hydrodynamic aspects of rollers and journal bearing [Dammak and Hadj-Taïeb (2010); Benmansour (1993); Nouar *et al.* (1996)]. Some works deal also with the effect of fluid flow on heat transfer mechanisms at the fluid-ring-rollers interfaces. Bejan's work (1990) is a reference for this aspect. Litsek *et al.* [(1990, 1991)] examine the fluid influence in a cavity constituted by two rotating cylinders. These works are however limited to a maximum Reynolds number $Re=400$ and cannot be used to understand thermal phenomena for high Re values corresponding to many applications. Recent works by Guenoun *et al.* [(2006, 2008)] explores a large range of Re including turbulent regime. This numerical work leads to the determination of dynamical and thermal fields in cavities limited by rollers and rings. The command of thermal exchanges within these cavities is useful for improving the efficiency, reliability and durability of these mechanisms. In the automotive field for example, the knowledge of fluid-solid heat transfer in thermal engines allows to optimize the global thermomechanical efficiency. This aspect has been treated in many works such as in Hocine *et al.* (2010). Several causes can be in the origin of bearings deterioration. Besides the thermal effects mostly due to friction between moving surfaces in contact, are the mechanical forces exerted on different parts of the bearing and the chemical reactions at solid-fluid interfaces causing corrosion. Bearing degradation may entail adverse effects on engine performance and thus on its reliability, which is unacceptable for example in the case of aircraft engines. Naeem *et al.* (1998) deal with the case of gas turbines and refer to the deterioration of thermal origin. The stability of rotor-bearing system is also linked to the proper operation of these mechanisms as shown by El - Marhomya *et al.* (2004). The mechanical stress suffered by the bearings commonly used in wind turbines can also greatly diminish their performance. The work by Audierne *et al.* (2010) and that of Melicio *et al.* (2011) address these issues. It is also the case of shafts of centrifugal compressors illustrated in the study

by Benini *et al.* (2007).

In the present study, the Nusselt number characterizing the heat transfer in the solid-fluid bearing interfaces is linked to the main physical and geometrical parameters of the system. Their respective influences are examined and new $Nu-Re-Pr$ correlations are proposed for two specific shape factors $A=2.5$ and 3.5 , corresponding to real rollers frequently used. These correlations are useful for the design and production of bearings widely used in mechanical assemblies which are especially sensitive to local thermal conditions along their operation. The proposed correlations concern a wide range of Re numbers and come to complement some published results that are valid only low Re numbers (laminar regimes). They can be applied to cylindrical roller bearings where the fluid flow is characterized by large Re values.

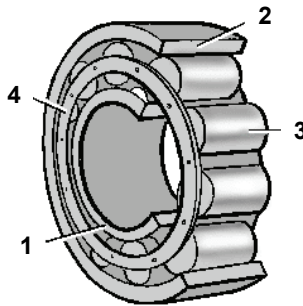


Figure 1: The treated roller bearing. 1. inner ring, 2. outer ring, 3. roller, 4. cage

2 Problem formulation

The treated cylindrical roller bearing represented in Fig. 1 is composed of an inner ring, an outer ring, cylindrical rollers and a cage. The thermal influence of the cage is neglected in the present study. The ring-rollers contacts represented in Fig. 2 (a) generate heat by friction that is evacuated essentially by convection between the fluid and the free surfaces of the solids. The heat flux is assumed as the same for all sectors of the bearing, so the considered problem is reduced to the single sector represented in Fig. 2 (b) by adopting a condition of angular periodicity. Studied cavity is thus limited by two cylindrical rolls, of radius R , submitted to a constant heat flux q . Their rotation at angular velocity ω is linked to the translation of both upper and lower walls representing the roller's rings at a constant velocity $V=\omega R$ as depicted in Fig. 2 (b). These walls are maintained at temperature T_0 . Angular reference is indicated in Fig. 2(c). Two specific shape factors are considered in

this work, $A=L/R=2.5$ and 3.5 , being L the distance between the rollers axis as indicated on the presented model. These values of A correspond to the real values of the studied rolls.

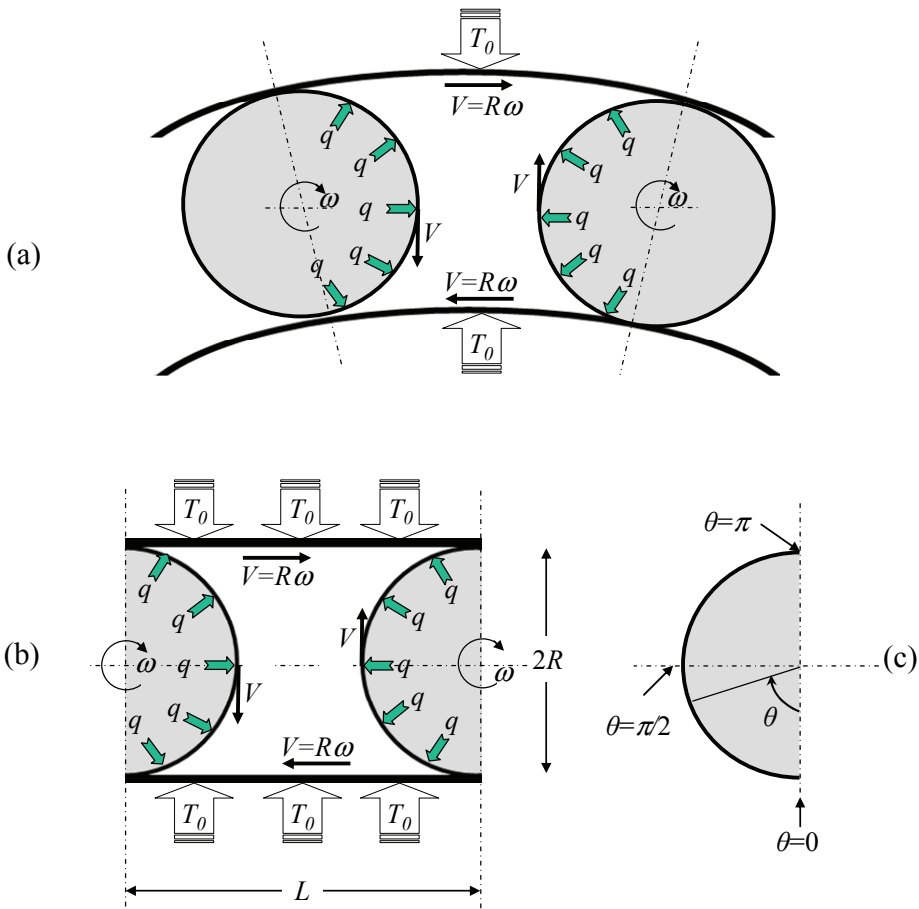


Figure 2: (a) Geometry of the treated cavity (b) studied model (c) angular reference

3 Governing equations, numerical solution and grid sensitivity testing

2D fluid flow is governed by the well known conservation equations

$$\frac{\partial U_i}{\partial X_i} = 0 \quad (1)$$

$$\rho U_i \frac{\partial U_j}{\partial X_i} = -\frac{\partial P}{\partial X_j} + \mu \frac{\partial^2 U_j}{\partial X_i^2} \quad (2)$$

$$\rho C_p U_i \frac{\partial T}{\partial X_i} = \frac{\partial}{\partial X_j} \left[\lambda \frac{\partial T}{\partial X_j} \right] + D \quad (3)$$

where U_i are the velocity components in the directions X_i . The viscous dissipation term D that appears in the energy equation (3) represents the viscous heat generation particularly important in this work, detailed in Litsek and Bejan (1990).

This system of equations is associated to the thermal and dynamic boundary conditions outlined in Fig. 2 (b) and described in Section 2. The fluid is viscous and adheres to the walls of the cavity (velocity nul). The viscous dissipation term in (3) is small for low-viscosity fluids like the air but it is very important for other fluids like water or specific oils used in bearing lubrication. This term is not neglected for any of the fluids considered in the present work and it deserves a special attention.

The dimensionless parameters used to get the solution are as follows:

the dimensionless fluid temperature

$$T^* = \frac{T - T_0}{\frac{qR}{\lambda}} \quad (4)$$

the dimensionless maximum temperature of the rollers

$$T_{\max,r}^* = \frac{T_{\max,r} - T_0}{\frac{qR}{\lambda}} \quad (5)$$

the Reynolds and Prandtl numbers

$$Re = \frac{VR}{\nu}; \quad Pr = \frac{\nu}{a} \quad (6)$$

the Nusselt number using the average temperature of the roller \overline{T}_r

$$Nu = \frac{\overline{T}_r - T_0}{\frac{qR}{\lambda}} \quad (7)$$

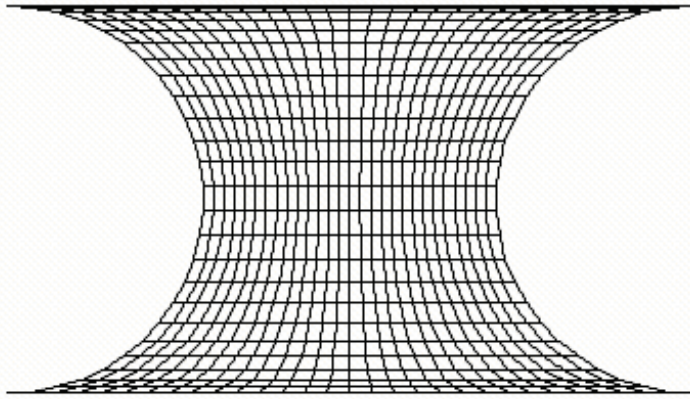


Figure 3: Mesh structure

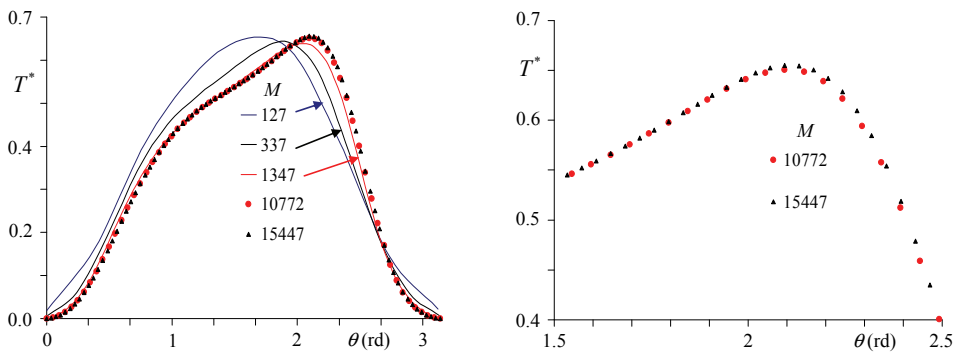


Figure 4: Influence of mesh on calculations for $A=3.5$ and $Re=1900$ (a) for $0 \leq \theta \leq \pi$ (b) detail for $1.5 \leq \theta \leq 2.5$

The value of Nu obtained in case of pure conduction, i.e. for the roller at rest, is denoted by Nu_0 . For the different configurations treated, the radius of the roller and the temperature of the rings are fixed and equal to $R=2$ cm and $T_0 = 500K$ respectively while the heat flux density q is variable between 10^3 and 10^5 Wm^{-2} . The velocity V is adjusted to give the wanted Reynolds number from Eq. (6). The average temperature of the roller \bar{T}_r is then determined what allows to obtain the Nusselt number from Eq. (7). A wide range of Re varying between 0 and 10^4 is considered. Many Pr numbers are also taken into account, whose values varying between 0.7 and 20 correspond to various fluids of engineering interest including

air, some gases at specific temperature and pressure conditions, water and some specific oils used in lubrication. The governing equations are solved by using the finite volume method described in several works as in Patankar (1980) and Versteeg *et al.* (1995). The adopted mesh structure is quadrangular as represented in Fig. 3. Discretisation is tight at the vicinity of the walls to properly deal with the boundary layer effects and is larger beyond. A specific investigation has been conducted in order to determine the optimum meshing ensuring the best ratio between results accuracy and calculation time. Dimensionless temperature T^* , considered representative of the problem, is taken into account for this preliminary mesh sensitivity study which indeed strongly depends on Re value. Many meshing tests have been carried out in order to determine the necessary number of elements M . The selected conditions correspond to the most unfavourable physic configuration. Results are illustrated for $Re=2900$ in Fig. 4 where T^* is represented versus θ for some M values and $A=3.5$. The resulting mean relative difference in T^* is less than 0.15% for $M=10772$ and $M=15447$. The difference is less than 0.01% between the mesh with $M=15447$ and a four times thinner mesh that requires about 22 times higher calculation time. Finally the value $M=10772$ is adopted for all calculations in the range $Re < 3000$ while 17244 elements become necessary for the range $3000 \leq Re \leq 10^4$. Calculations are done in steady state regime. The first 200 iterations constitute the most delicate stage of calculations. Convergence is very sensitive to the initial iterative process which is optimized to limit the computation time. The criteria of convergence adopted in the numerical procedure are based on the velocity and energy, applied to all control volumes. The iterative process is stopped when the relative differences between the results of two successive iterations are lower than 10^{-5} for the velocity components and 10^{-6} for the energy. Turbulence is modelled by using the well-known $k-\varepsilon$ approach developed in Launder *et al.* (1974) that is appropriate for the present study.

4 Results

Distribution of Nusselt number for air ($Pr=0.7$) is given in Fig. 5 for the entire studied range of Re and two specific values of the aspect ratio $A=2.5$ and 3.5. Nusselt number values are systematically higher for $A=3.5$ both in laminar and turbulent regimes. The influence of this important parameter has been treated in various studies concerning convection in enclosures, whether it is forced like here or in natural convection. Studies [Bejan (2004); Baïri *et al.* (2007); Baïri (2008); Semma *et al.* (2006)] for example, show the influence of A on free convective exchanges for several thermal and dynamic conditions, depending on the treated geometrical configuration. It is thus necessary to study this aspect for every considered case. The number of rollers which is directly linked to A , has to be wisely chosen in

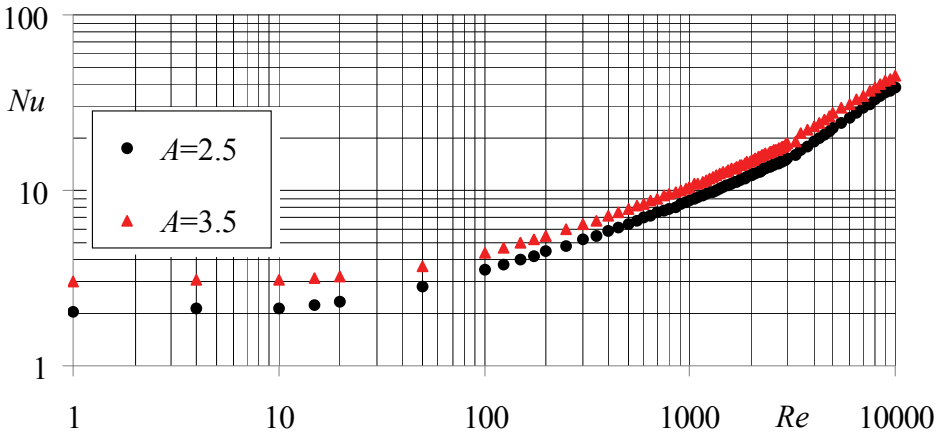


Figure 5: Variation of Nu versus Re for $A=2.5$ and 3.5 with $Pr=0.7$.

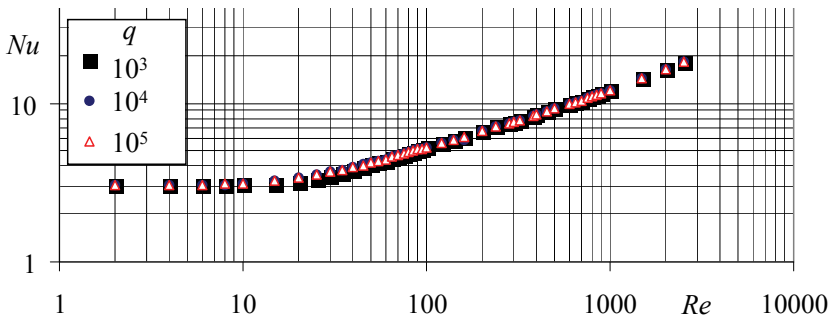


Figure 6: Variation of Nu versus Re in the laminar zone for $A=3.5$ and different values of q . $Pr=0.7$.

order to avoid extreme thermal gradients which would cause roller malfunction. Nusselt number is calculated for various thermal boundary conditions, based on q and T_0 values. Results presented in Fig. 6 for $Pr=0.7$ and $A=3.5$ demonstrates Nu invariance for a wide range of Re and three specific values of $q=10^3, 10^4$ and 10^5 Wm^{-2} . Values of Nu_0 corresponding to the Nu value when the mechanism is at rest, i.e. pure conduction condition, have been calculated for air ($Pr=0.7$). Results are in good agreement with those of Litsek and Bejan (1990) valid for $Pr=1$ being Re limited to 400. This is presented in Table 1 for $q=10^3 \text{ Wm}^{-2}$ showing small deviations, of about 0.5% and 2.3% for $A=2.5$ and 3.5 respectively.

Table 1: Values of Nu_0 for $A=2.5$ and 3.5 with $q=10^3 \text{ Wm}^{-2}$. Comparison between the results of the present study ($Pr=1$) with those of Litsek and Bejan (1990) ($Pr=1.0$)

A	2.5	3.5
This study ($Pr=0.1$)	2.01	2.97
Ref Litsek and Bejan (1990) ($Pr=1$)	2.00	2.90
Deviation (%)	0.5%	2.3%

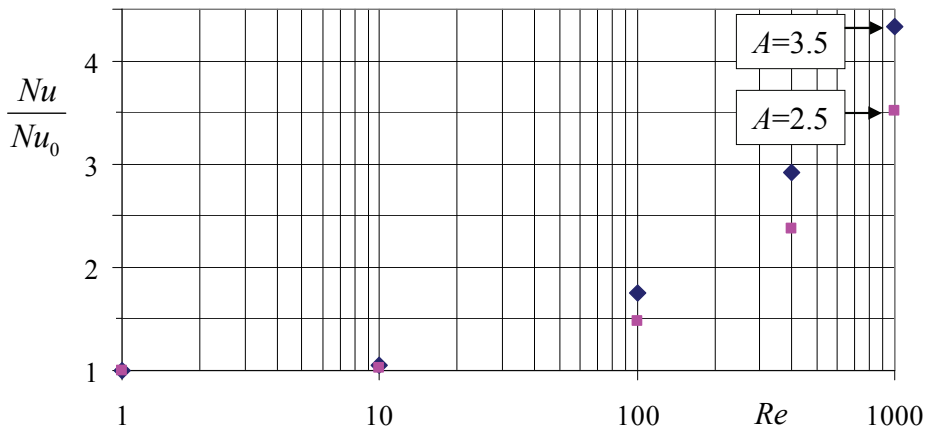


Figure 7: Variation of Nu/Nu_0 versus Re for $A=2.5$ and 3.5 . $Pr=0.7$.

To examine the influence of angular velocity on convective exchanges, Nusselt number Nu is compared to Nu_0 for several Pr numbers. Distribution of the Nu/Nu_0 ratio versus Re for $Pr=1$ is presented in Fig. 7 for the two shape factors $A=2.5$ and 3.5 . Starting from $Re=10$, the Nu/Nu_0 ratio increases with Re , confirming that convection is dominating in the enclosure when velocity increases. Values are higher for $A=3.5$ as noted previously. A comparison between these results for $Pr = 0.7$ and those of Litsek and Bejan (1990) for $Pr = 1$ is presented in Fig. 8 for $A=2.5$. Concordance is good for these two similar values of Pr , deviation being about 4.5% for $A=3.5$. Thermal exchanges are also quantified through the temperature fields. Fig. 9 illustrates the dimensionless temperature distribution T^* on left roller's surface for $A=2.5$ and several values of Re , for $Pr=1$. For very low rotation velocities, for example for $Re=1$, the peak of temperature is almost centred at $\theta=\pi/2$, being the temperature profile symmetric on the roller. This peak moves away between $\theta=\pi/2$ and $\theta=\pi$ as Re increases, and T^* becomes almost uniform for high values of Re . Distribution of $T_{\max,r}^*$ is given in Fig. 10 versus Reynolds number for both treated

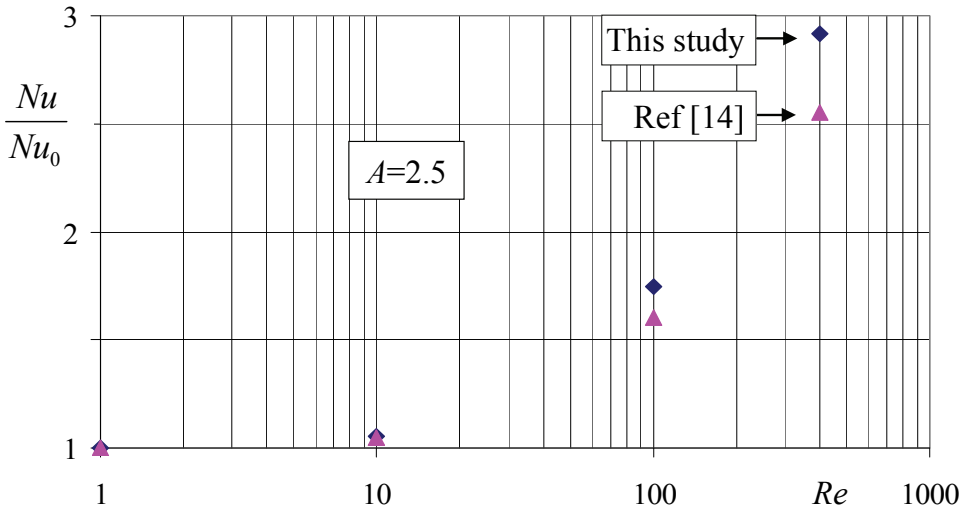


Figure 8: Variation of Nu/Nu_0 versus Re for $A=2.5$ and $Pr=1$. Comparison between present study and Litsek and Bejan (1990) ($Pr=1$)

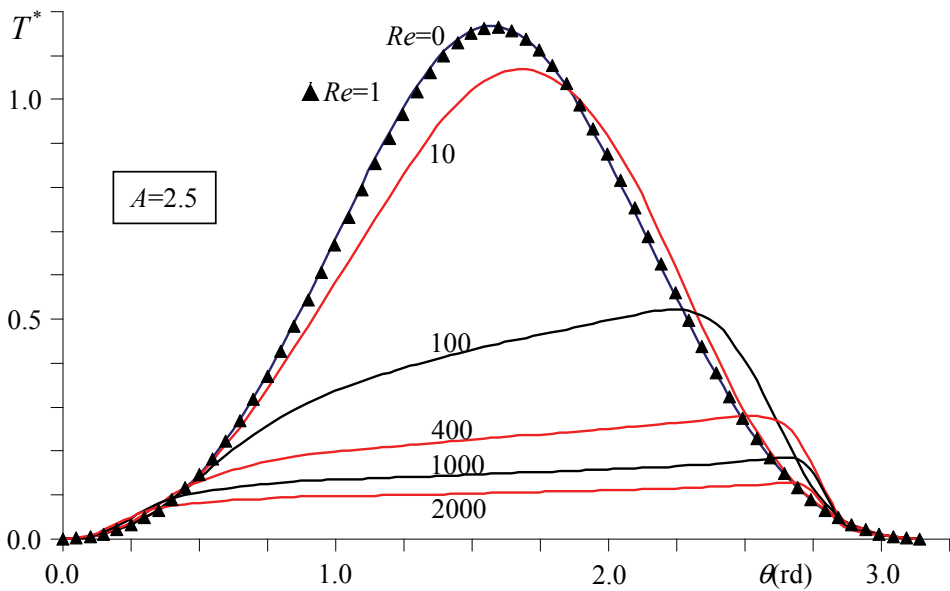


Figure 9: Distribution of T^* on the surface of the left roller for $A= 2.5$ and various Re . $Pr=0.7$

shape factors A and for $Pr=1$. Note that in the treated range of Re , this maximum temperature regularly decreases when Re and A increase. The comparison between results of this study with those from Litsek and Bejan (1990) for $A=2.5$ and $Pr=1$ is given in Table 2 and shows a good concordance. The largest deviation (3.8%) remains very low since it corresponds to a bearing that is almost stopped ($Re=1$) and thus convection is very small.

Table 2: Values of $T_{\max,r}^*$ on the surface of the left roller versus Re for $A=2.5$ and $Pr=1$. Comparison between the results of the present study with those of Litsek and Bejan (1990).

Re	Ref Litsek and Bejan (1990)	Present study	Relative difference (%)
1	1.001	1.041	3.8
10	0.950	0.978	2.9
100	0.490	0.502	2.4
400	0.310	0.318	2.5

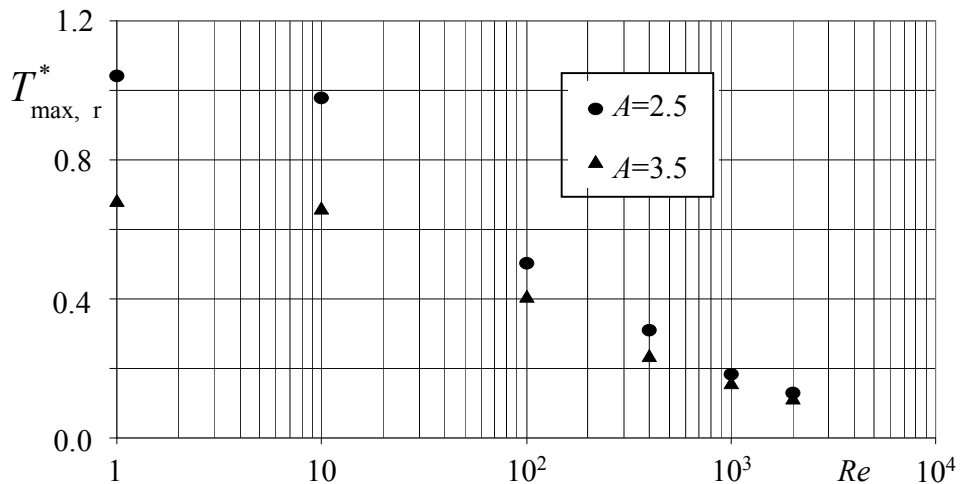


Figure 10: Distribution of $T_{\max,r}^*$ versus Re on the surface of the left roller. $A=2.5$ and 3.5 ; $Pr=0.7$.

Temperature peak shift due to rotational velocity results in a migration of hotter points, and thus in thermal spots appearing on roller's surface. This is presented for the previous case in Fig. 11 on which hot spot location is plotted versus Re for $A=2.5$ and 3.5 . Migration is eased by fluid rotation increase. The comparison with

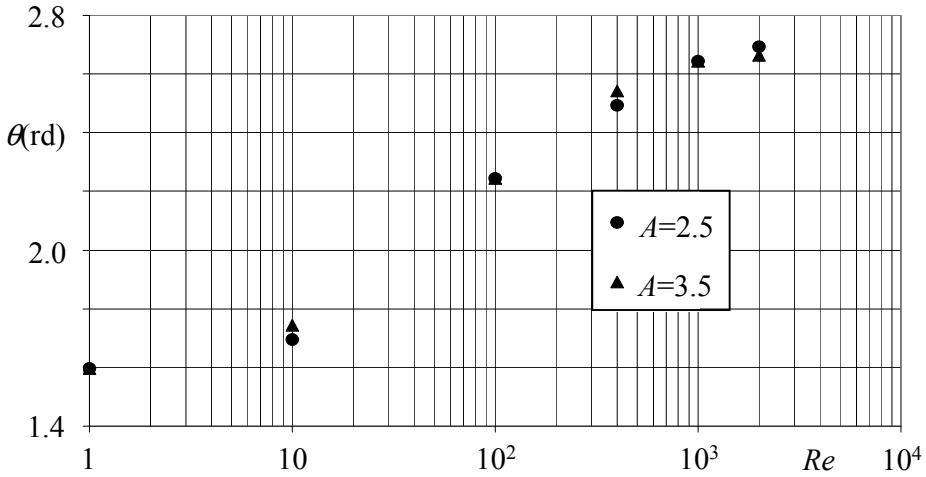


Figure 11: Angular position of $T_{\max,r}^*$ on the surface of the left roller. $A=2.5$ and 3.5 ; $Pr=0.7$

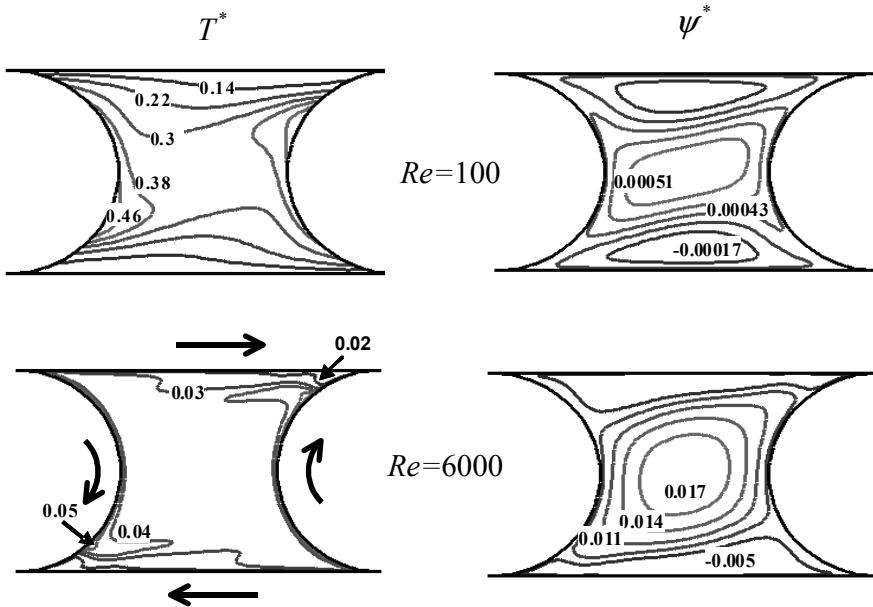


Figure 12: Isotherms T^* and streamlines ψ^* in the cavity. $A=3.5$; $Re=100$ and 6000 ; $Pr=0.7$

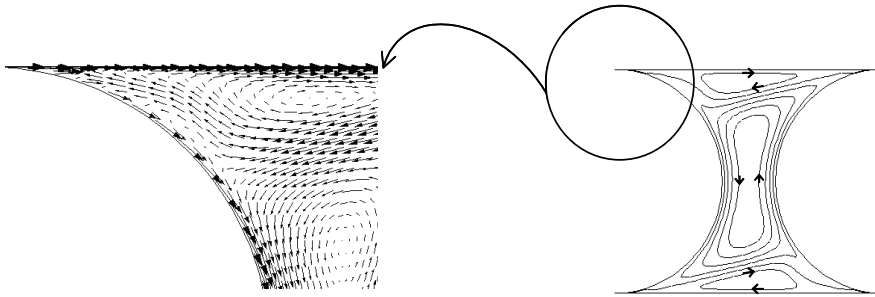


Figure 13: Fluid recirculation regions in the enclosure

results from Litsek and Bejan (1990) presented in Table 3 for $A=2.5$ shows again a good concordance between both studies.

Table 3: Values of θ (rd) corresponding to $T_{\max,r}^*$ on the surface of the left roller versus Re for $A=2.5$ and $Pr=1$. Comparison between the results of the present study with those of Litsek and Bejan (1990)

Re	Ref Litsek and Bejan (1990)	Present study	Deviation (%)
1	1.605	1.596	0.6
10	1.690	1.695	0.2
100	2.250	2.244	0.3
400	2.460	2.493	1.4

Isotherms T^* and streamlines ψ^* are presented in Fig. 12 for $A=3.5$, $Pr=0.7$ and two Reynolds numbers $Re=100$ and 6000 . Streamlines highlight the dissymmetry produced by rollers' rotation. This dissymmetry increases with velocity and thus with Re value. The same phenomenon is observed for the isotherms, with a strong evolution of the thermal boundary layer with Re . Two regions with strong thermal perturbations appear when Re increases, localized in the corners where fluid is brought by mobile walls. This phenomenon is intensified for $Re=6000$. Rollers' rotation and ring walls' translation boost the fluid recirculation regions in the enclosure as illustrated in Fig. 13.

5 Correlations

Several configurations have been treated by varying the main physical parameters. Results concerning Nusselt number distribution have been treated and analyzed for both outstanding Reynolds ranges corresponding to laminar and turbulent regimes.

To quantify convective exchanges in the enclosure, an investigation has been conducted in order to establish correlations of the following type

$$Nu = Nu_0 + k.A^p Re^n Pr^s \tag{8}$$

which leads to:

$$\ln(Nu - Nu_0) = \ln k + p \ln A + n \ln Re + s \ln Pr \tag{9}$$

A linear system is obtained, consisting on four equations corresponding to different numerical tests in which $(Nu - Nu_0)$, A , Re and Pr are fixed, allowing to determine the four constants k, p, n and s . The well known least squares method applied in [Guenoun (2008), Bauzin et al. (2008)] is implemented to minimize the function

$$J = \sum_{i=1}^T \left[\ln(Nu - Nu_0)_{i,or} - \ln(Nu - Nu_0)_{i,c} \right]^2 \tag{10}$$

In this equation, the term $(Nu - Nu_0)_{i,or}$ corresponds to the original values calculated with the numerical study, while the term $(Nu - Nu_0)_{i,c}$ is determined from Eq. (9) for the i^{th} test. Calculations are made for both cavity shape factors $A=2.5$ and 3.5 , corresponding to real rollers. Many Pr number are considered, with values varying between 0.7 and 20 corresponding to various fluids of engineering interest including air, some gases at specific temperature and pressure conditions, water and some specific oils.

The correlations finally obtained are:

$$Nu - Nu_0 = \begin{cases} 0.150 Re^{0.6} Pr^{0.7} & \text{for } 0 \leq Re \leq 3.10^3 \\ 0.031 Re^{0.8} Pr^{0.7} & \text{for } 3.10^3 \leq Re \leq 10^4 \end{cases} \tag{11}$$

$$\text{with } Nu_0 = \begin{cases} 1.9 & \text{for } A = 2.5 \\ 3.0 & \text{for } A = 3.5 \end{cases}$$

Valid for $0.7 \leq Pr \leq 20$.

They are obtained with correlation coefficients higher than 0.989 . Results issued from direct numerical calculations of this study have been compared with those given by these correlations. Average deviation are small, about 3.9% for $0 \leq Re \leq 3 \times 10^3$ and 5.7% for $3 \times 10^3 \leq Re \leq 10^4$. These results clearly show that the change of Nu is independent of the shape factor considered in this work. Only Nu_0 values, corresponding to bearing at rest, differ for both values of A . Comparison with results of Litsek and Bejan (1990) corresponding to low values of Re shows a good concordance.

6 Conclusion

This work examines convection in the enclosure limited by rollers and rings of a cylindrical roller bearing. The numerical study is accompanied by a mesh sensitivity study. Results show the influence of Re , A and Pr on convective heat transfer. Thermal spots on the roller's surface migrate from the centre of the roller to the contact region between the rings and the roller. This migration, consequence of the fluid flow, is highlighted by recirculation zones. The proposed $Nu-Re-Pr$ correlations are given for two shape factors of the enclosure and different fluids of engineering interest including air, water, and a specific oil. They cover a wide range of Re corresponding to real engineering applications and complete the results published in the literature, which are valid for a more limited range.

References

- Audierne, E.; Elizondo, J.; Bergami, L.; Ibarra, H.; Probst, O.** (2010): Analysis of the furling behavior of small wind turbines. *Applied Energy*, vol. 87, pp. 2278–2292.
- Baïri, A.; Alilat, N.; Bauzin, J. G.; Laraqi, N.** (2004): Three-dimensional stationary thermal behavior of a bearing ball. *Int. J. Thermal Sciences*, vol. 43, pp. 561-568.
- Baïri, A.; Garcia-De Maria, J.M.; Laraqi, N.** (2004): Effect of thickness and physical properties of films on the thermal behavior of a moving rough interface. *Eur. Phys. J- Appl. Phys.*, vol. 26, pp. 29-34.
- Baïri, A.; Laraqi, N.; Garcia de Maria, J.M.** (2007): Numerical and experimental study of natural convection in tilted parallelepipedic cavities for large Rayleigh numbers. *Experimental Thermal and Fluid Science*, vol. 31, pp. 309-324.
- Baïri, A.** (2008): Nusselt-Rayleigh correlations for the design of industrial elements: experimental and numerical investigation of natural convection in tilted square air-filled enclosures. *Energy Conversion and Management*, vol. 49, pp. 771-182.
- Bauzin, J.G.; Laraqi, N.; Baïri, A.** (2008): Estimation of thermal contact parameters at the interface of two sliding bodies. *Journal of Physics-Conf. series*, vol. 135, paper n° 012015.
- Bejan, A.** (1989): Theory of rolling contact heat transfer. *ASME Journal of Heat Transfer*, vol. 111, pp. 257-263.
- Bejan, A.** (2004): *Convection heat transfer*, 3rd Edition, ISBN 978-0-471-27150-5, Wiley.
- Belghazi, H.; El Ganaoui, M.; Labbe, J.C.** (2010): Analytical solution of un-

steady heat conduction in a two-layered material in imperfect contact subjected to a moving heat source. *Int. J. Therm. Sciences*, vol. 49, pp. 311–318.

Benini, E.; Giacometti, S. (2007): Design, manufacturing and operation of a small turbojet-engine for research purposes. *Applied Energy*, vol. 84, pp. 102–1116.

Benmansour, I. (1993) : *Etude des écoulements confinés entre parois mobiles : application aux roulements*. Ph.D. thesis Thèse de Doctorat de l'Université Paris 6.

Briot, J.M. (2001) : Influence de la vitesse et de la charge sur la conductance thermique de transport entre les bagues d'un roulement à rouleaux. PhD thesis, Université Nantes, France.

Dammak, L.; and HadjTaieb, E. (2010): Finite Element Analysis of Elastohydrodynamic Cylindrical Journal Bearing. *Fluid Dyn. Mater. Process*, vol. 6, no. 4, pp. 419-430.

El-Marhomya, A. A.; Abdel-Sattarb, N.E. (2004): Stability analysis of rotor-bearing systems via Routh-Hurwitz criterion, *Applied Energy*, vol. 77, pp. 287–308.

Fruman, D.H.; Benmansour, I.; Nouar, C.; Bidot, T.; Vane, J.M. (1996): Analytical, numerical and experimental investigation of the flow structure in a flooded ball bearing, *ASME J. Tribology*, vol. 118, pp. 865-871.

Gecim, B.; Winer, W.O. (1986): Steady temperatures in a rotating cylinder. Some variations in the geometry and the thermal boundary conditions. *ASME Journal of Tribology*, vol. 108, pp. 446-454.

Guenoun, S. ; Baïri, A. ; Laraqi, N. (2006) : Convection dans l'entrefer rouleaux-bagues d'un roulement. *Proceedings of Congrès annuel de la Société Française de Thermique (SFT)*, Elsevier, 16-19 may 2006, Ile de Ré, France.

Guenoun. S. (2008) : *Transfert thermique dans les dispositifs mécaniques soumis aux frottements. Modélisation et expérimentation*, Ph.D. thesis, University Paris 10, France.

Hocine, A.; Desmet, B.; Guenoun, S. (2010): Numerical study of the influence of Diesel post injection and exhaust gas expansion on the thermal cycle of an automobile engine, *Applied Thermal Engineering*, vol. 30, pp. 1889-1895.

Laraqi, N. (2010): Thermal impedance and transient temperature due to a spot of heat on a half-space. *Int. J. Thermal Sciences*, vol. 49, pp. 529-533.

Laraqi, N.; Bounagui, A.; Bransier, J. (1994): Modélisation des transferts de chaleur dans un roulement à rouleaux cylindriques. *Revue Française de Mécanique*, vol. 3, pp. 223-227.

Lauder, B.E.; Spalding, D.B. (1974): The numerical computation of turbulent flows. *Computer Methods in Applied Mechanics and Engineering*, vol. 3, pp. 269–

289.

Litsek, P.A.; Bejan, A. (1990): Convection in the cavity formed between two cylindrical rollers, *ASME Journal of Heat Transfer*, vol. 112, pp. 625-631.

Litsek, P.A.; Zhang, Z.; Bejan, A. (1991): Convection in the cavity between two rollers: the effect of thermal boundary conditions. *ASME Journal of Heat Transfer*, vol. 113, pp. 249-251.

Melício, R.; Mendes, V. M. E.; Catalão, J. P. S. (2011): Transient analysis of variable-speed wind turbines at wind speed disturbances and a pitch control malfunction. *Applied Energy*, vol. 88, pp. 1322–1330.

Naeem, M.; Singh, R.; Probert, D. (1998): Implications of engine deterioration for creep life, *Applied Energy*, vol. 60, pp.183-223.

Nouar, C.; Fruman, D.H.; Gaudemer, R. (1996): Flow structure in a flooded ball bearing. *Experiments in Fluids*, vol. 21, pp. 71-79.

Patankar, S.V. (1980): *Numerical heat transfer and fluid flow*. Taylor and Francis.

Patula, E. J. (1981): Steady state temperature distribution in a rotating roll subject to surface heat fluxes and convective cooling. *ASME Journal of Heat Transfer*, vol. 103, pp. 36-41.

Semma, E.A.; El Ganaoui, M.; Timchenko, V.; Leonardi, E. (2006): Some Thermal Modulation Effects on Directional Solidification. *Fluid Dynamics and Materials Processing*, vol. 2, no. 3, pp. 191-202.

Versteeg, H.K.; Malalasekera, W. (1995): *Computational fluid dynamics, the finite volume method*, Pearson Education, Limited.